energies

MDPI

Article

Impact on Thermal Energy Needs Caused by the Use of Different Solar Irradiance Decomposition and Transposition Models: Application of EN ISO 52016-1 and EN ISO 52010-1 Standards for Five European Cities

Serena Summa *, Giada Remia, Ambra Sebastianelli, Gianluca Coccia and Costanzo Di Perna

Industrial Engineering and Mathematical Sciences Department, Università Politecnica delle Marche, Via Brecce Bianche 1, 60131 Ancona, Italy
* Correspondence: s.summa@univpm.it

Abstract: To solve the series of heat balances that EN ISO 52016-1 uses to simulate the dynamic hourly energy requirements of a building, detailed climatic data are required as input. Differently from air temperatures, relative humidity and wind speed, which are easily measurable and available in databases, the direct and diffuse solar irradiances incident on the different inclined and oriented surfaces, which are fundamental for the evaluation of solar gains, must be estimated using one of the many regression models available in the literature. Therefore, in this work, the energy needs of buildings were evaluated with the simplified hourly dynamic method of EN ISO 52016-1 by varying the solar irradiance sets on inclined and oriented surfaces obtained from EN ISO 52010-1 and three other pairs of solar irradiance separation and transposition models. Five European locations and two different window solar transmission coefficients (g_{gl}) were analysed. The results showed that on average, for the heating period and for both g_{gl}, the use of the different methods causes an average error on the calculation of the annual demand of less or slightly more than 5%; while for the cooling period, the average error on the calculation of the annual demand is 16.4% for the case study with g_{gl} = 0.28 and 25.1% for the case study with g_{gl} = 0.63. On the other hand, analysing the root-mean-square-error of the hourly data, using the model contained in TRNSYS as a benchmark, for most of the cases, when varying window orientations, cities and g_{gl}, the model that diverges furthest from the others is that contained in EN ISO 52010-1.

Keywords: EN ISO 52016-1; EN ISO 52010-1; solar irradiance decomposition and trasposition models; climate data; building simulation; building energy performance

Citation: Summa, S.; Remia, G.; Sebastianelli, A.; Coccia, G.; Di Perna, C. Impact on Thermal Energy Needs Caused by the Use of Different Solar Irradiance Decomposition and Transposition Models: Application of EN ISO 52016-1 and EN ISO 52010-1 Standards for Five European Cities. *Energies* **2022**, *15*, 8904. https://doi.org/10.3390/en15238904

Academic Editors: Bin Chen, Teng Shao, Yu Liu and Wuxing Zheng

Received: 25 October 2022
Accepted: 21 November 2022
Published: 25 November 2022

1. Introduction

To date, buildings and their construction account for more than a third of the World's final energy consumption and almost 40% of total CO_2 emissions [1]. In fact, around 35% of buildings in the EU are over 50 years old, 75% of the building stock is energy inefficient and the annual renovation rate is just 1% [2]. To promote energy-conscious design, the European Committee for Standardisation (CEN) approved a new set of standards (called 'EN ISO 52000 family' [3]) that provided member states with adequate computational tools to be able to assess the real energy performance of buildings, both at the design and energy requalification stages.

These standards aim at international harmonisation of the methodology for assessing the energy performance of buildings by offering a systemic and holistic approach that considers the dynamic interaction between systems, users and climatic conditions. Of them all, EN ISO 52016-1:2017 [4] is the one that introduces the dynamic hourly method for calculating heating and cooling energy needs, indoor temperatures and sensible and latent heat loads, requiring a limited number of input data and ensuring reproducibility

and transparency of calculation [5]. This standard, which is proposed as an alternative to the use of the main simulation software, has recently generated interest from the scientific community, which has begun to evaluate its accuracy. Ballarini et al. [6], comparing the standard's method with Energy Plus, highlighted a discrepancy in terms of thermal loads attributable to the use of different surface heat transfer coefficients and a different modelling of extra thermal radiation to the sky. Zakula et al. [7], through a comparative analysis with TRNSYS, showed a difference in results caused by the use of constant values of the thermal transmittance of glazed surfaces (F_w), the use of constant values of the solar transmission coefficient (g_{gl}) and to a lesser extent by the heat transfer pattern of opaque elements. With regard to the latter problem, Mazzarella et al. [8] analysed and compared with both TRNSYS and the analytical solution, the model implemented in the Italian National Annex that proposes an alternative method for defining the RC network of opaque elements based on the thermo-physical characteristics of each individual layer that makes up the building element. The use of this model reduced the error on the amplitude of the internal flux by up to 67% and generated an average error on the external flux of only 3% compared to the heat transfer model of opaque surfaces proposed in standard in EN ISO 52016-1. As for the heat transfer model of opaque elements, the problem of using constant values of the solar transmission coefficient (g_{gl}) was also improved.

In the study by Summa et al. [9], a model (also implemented in the Italian National Annex of EN ISO 52016-1) was tested to calculate an hourly solar transmission coefficient as a function of the angle of incidence of solar radiation, but also as a function of the number of glass panels of the window and the type of glass coating (float glass, low emissivity, solar control, etc.). The results obtained, using TRNSYS as a baseline, showed a 47% improvement in the root-mean-square deviation (RMSE) of summer solar loads (thermal loads caused by solar radiation entering from glazed surfaces) compared to the method proposed by the standard EN ISO 52016-1 with constant g_{gl}. These results were also confirmed in study [10], where it is affirmed that the use of hourly g_{gl} correction factors resulted to be the most sensitive modelling option, among those analysed. As can be observed from the literature studies, EN ISO 52016 [4] shows some discrepancies in terms of energy requirements compared to the main dynamic simulation software (i.e., Trnsys, Energy Plus), but researchers are analysing and proposing improvements to the algorithm, limiting the demand for new input data from designers, which could introduce subjective uncertainty and inaccuracy into the calculation [11].

However, the results of dynamic energy simulations are influenced not only by the calculation models, but also by the accuracy of the hourly variables required as input to EN ISO 52016 [4] and from additional calculation algorithms, such as climatic data. The meteorological parameters, such as dry bulb temperature, relative humidity, solar irradiance, wind speed and direction, are in fact those that have the greatest influence on the energy balance of a building [12,13], and among these, solar irradiance is the most impactful phenomenon [14]. Differently from the other meteorological parameters that are directly measured and present in the Typical Meteorological Years (TMY/TMY2), the measured solar radiation is only the global horizontal radiation (for TMY) and in some cases also the direct normal irradiation (for TMY2). In order to reconstruct diffuse, direct and global irradiance data for all surfaces with arbitrary tilt and orientation, auxiliary calculation methods are needed. To overcome this problem, CEN decided to introduce a single consistent source for all energy performance of buildings standards for the conversion of climate data for energy calculations [15], i.e., EN ISO 52010-1:2017 [16]. This standard allows to calculate the hourly solar irradiance on a surface with arbitrary orientation and inclination from measurements of global horizontal irradiance, temperature, humidity, solar constant, albedo and geographical coordinates of the site. Few studies exist in the literature that attempt to validate EN ISO 52010-1 [16]. In [17], a comparative analysis of four different models for the calculation of direct and diffuse irradiance on arbitrarily inclined and oriented surfaces was performed for five European cities. The results showed that, in comparison to the models implemented in TRNSYS, the model implemented in EN ISO

52010 [16] is the one that mostly overestimates the diffuse solar irradiance on the horizontal plane and underestimates the annual direct irradiance on south, west, east and north facing surfaces by 24.2%, 55.9%, −0.9% and 69.4% respectively. In [18], instead, through the monthly quasi-steady-state method of EN ISO 13790 [19], the energy performance of two typical residential buildings in five Polish cities was calculated, using as input the solar irradiance on inclined and oriented surfaces obtained from 15 different calculation models, including that of EN ISO 52010 [16]. Taking as baseline the TMYs containing irradiances on sloping surfaces with five slope angles and oriented in eight directions, it was seen that the use of EN ISO 52010 [16] introduces a difference on the energy performance indicator for heating, domestic hot water and ventilation (EPH+W) of 1.6 and 1.2 kWh/m^2 for the single-family building, respectively, for the use of a g_{gl} = 0.75 and g_{gl} = 0.50, and a difference of 5.1 and 3.9 kWh/m^2 for the multi-family building, varying its energy classification. Therefore, in order to extend the knowledge of these issues, in this research a comparative analysis of the solar loads and heating and cooling energy needs calculated with the simplified hourly dynamic method of EN ISO 52016-1 [4] will be carried out for the first time, varying the solar irradiance sets on inclined and oriented surfaces obtained from EN ISO 52010 [16] and three other pairs of solar irradiance separation and transposition models. The simulations will be conducted for five European locations, on a cubic building, changing each time the orientation of the glazed surface and the solar transmission coefficient (g_{gl}).

After this Introduction, this paper will follow with Section 2 describing the Methodology, Section 3 illustrating the Case Study, Section 4 discussing the Results and finally Section 5 with the main conclusions and future developments.

2. Methods

Energy requirements obtained from hourly dynamic simulations performed with EN ISO 52016-1 [4] were compared by varying the input solar irradiances on inclined and oriented surfaces simulated with four different algorithms including the one contained in EN ISO 52010-1:2017 [16].

Both of the above-mentioned standards are part of the new series of standards called EPB 'Energy Performance of Buildings', which aim at international harmonisation of the methodology for assessing the energy performance of buildings, from the identification of input data to the calculation of primary energy (see Figure 1).

EN ISO 52016-1 [4] potentially allows hourly dynamic calculations of heating and cooling energy needs, indoor air temperatures, mean radiant temperatures of the surfaces enclosing the heated thermal zone and operative temperatures of individual thermal zones in the building, in a simplified way, but with accuracy similar to the main simulation software (TRNSYS 17, Energy+ 9.6.0, etc.).

EN ISO 52010-1 [16], starting from the geographical coordinates and the hourly horizontal global irradiance of the site, allows to obtain the direct and diffuse irradiances on any surface with arbitrary orientation and inclination. These irradiances are those required by EN ISO 52016-1 [4] for building energy calculations but can also be used in standards for the design/verification of technical building system components, such as solar thermal collectors and photovoltaic panels. In addition to EN ISO 52010-1 [16], three other algorithms for splitting direct and diffuse radiation, previously compared in [17], were used, i.e., the one implemented: (i) in the work of Summa et al. [17], that makes modifications to the UNI 10349-1:2016 standard [20], (ii) in Meteonorm software [21] and (iii) that implemented in Type 16c of the TRNSYS software [22]. The models used by each algorithm for the split between direct and diffuse radiation are shown in Table 1.

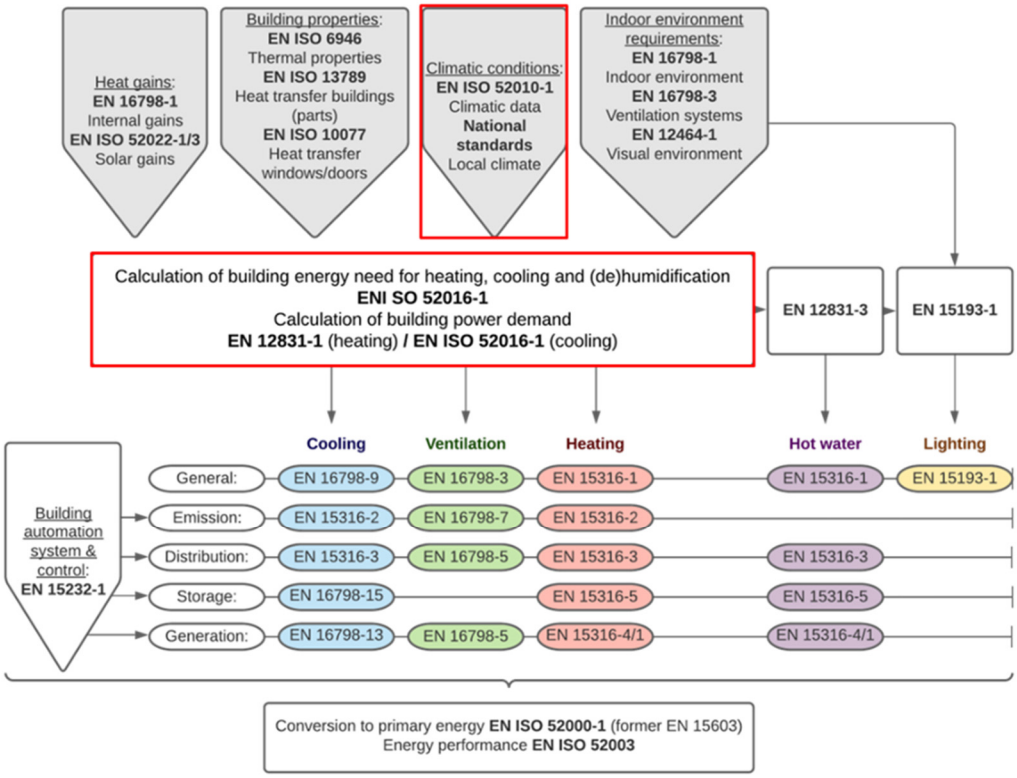

Figure 1. New set of standards denominate EPB "Energy Performance of Buildings". The standards used in this study are highlighted in red.

Table 1. Models for the calculation of direct and diffuse solar radiation for each algorithm tested. The asterisk * used beside "Perez et al. 1990 *" indicates the change in EN ISO 52010 [16] from the classical method of Perez et al. 1990 on the calculation of the "dimensionless clarity parameter" (see Formula (11)).

	Abbreviation	Decomposition Model	Trasposition Model
Summa et al. [17]	B-L	Boland et al. 2007 [23]	Liu et al. 1960 [24]
En Iso 52010 [16]	E-P*	Erbs et al. 1982 [25]	Perez et al. 1990 * [26]
Meteonorm 7.3 [21]	P-P	Perez et al. 1991 [27]	Perez et al. 1990 [26]
TRNSYS 17 [22]	R-P	Reindl et al.1990 [28]	Perez et al. 1990 [26]

The Boland et al. model [23] is used to calculate the diffuse solar irradiance on horizontal plane $G_{sol;d}$ (W/m^2) as follows:

$$G_{sol;d} = \frac{1}{1 + e^{-5+8.6k_{T,d}}} \cdot G_{sol;g}, \quad (1)$$

where

$k_{T,d} = \frac{G_{sol;g}}{I_{ext,h}}$ is the clearness index of the atmosphere (relating to diffuse radiation).

$G_{sol;g}$ is the global horizontal solar irradiance (climatic data set) (W/m^2).

$I_{ext,h} = I_{ext} \cdot \sin \alpha_{sol}$ is the global extra-atmospheric solar irradiance on a horizontal plane (W/m^2).

I_{ext} is extra-terrestrial radiation (W/m^2).

α_{sol} is solar altitude angle (°).

The Erbs et al. model [25] is used to calculate the diffuse solar irradiance on horizontal plane $G_{sol;d}$ (W/m^2) as follows:

$$\text{If} \quad k_T \leq 0.22 \quad \rightarrow G_{sol;d} = (1.0 - 0.09 \cdot k_T) \cdot G_{sol;g}, \quad (2)$$

$$\text{If} \quad 0.22 < k_T \leq 0.80 \rightarrow G_{sol;d} = \left(0.9511 - 0.1604 \cdot k_T + 4.388 \cdot {k_T}^2 - 16.638 \cdot {k_T}^3 + 12.336 \cdot {k_T}^4\right) \cdot G_{sol;g}, \tag{3}$$

$$\text{If} \quad k_T > 0.80 \rightarrow G_{sol;d} = 0.1655 \cdot G_{sol;g}, \tag{4}$$

where

$k_T = \frac{G_{sol;g}}{I_{ext}}$ is the clearness index of the atmosphere (relating to beam radiation).

The Perez et al. 1991 model [27] is used to calculate the normal solar irradiation $G_{sol;n}$ (W/m^2) as follows:

$$\text{Method (1)} \quad G_{sol;n} = I_{DISC} \cdot X\left(k'_t,\ Z,\ W,\ \cdot k'_t\right), \tag{5}$$

where

I_{DISC} is direct normal irradiation estimate by the DISC model (itself a function of global irradiance and solar zenith angle) [29].

$X\left(k'_t,\ Z,\ W,\ \cdot k'_t\right)$ are obtained from 4-dimensional look-up table based on the bins in Table 1 of paper [30].

$k'_t = \frac{k_T}{\left(1.031 \cdot \exp\left(\frac{-1.4}{0.9 + \frac{9.4}{m}}\right) + 0.1\right)}$ is the clearness index based on Kasten's 1980 [31].

m is the relative optical air mass from Kasten 1966 [32].

Z is solar zenith angle (°).

$W = \exp(0.07 \cdot T_d - 0.075)$ is the atmospheric precipitable water [33].

T_d is ground dew-point temperature (°C).

$\Delta k'_t = 0.5 \cdot \left(\left|k'_t - k'_{t+1}\right| + \left|k'_t - k'_{t-1}\right|\right)$ is "stability index" [34].

$$\text{Method (2)} \quad G_{sol;n} = I_{ext} \cdot k'_b \cdot \exp\left(\frac{-1.4}{0.9 + \frac{9.4}{m}}\right) \cdot \frac{1}{0.87291}, \tag{6}$$

where

if $k'_t < 0.2 \rightarrow k'_b = 0$.

otherwise $k'_b = a\left(k'_t,\ Z,\ W,\ \Delta k'_t\right) \cdot k'_t + b\left(k'_t,\ Z,\ W,\ \Delta k'_t\right)$.

$a\left(k'_t,\ Z,\ W,\ \Delta k'_t\right)$ and $b\left(k'_t,\ Z,\ W,\ \Delta k'_t\right)$ are obtained from 4-dimensional look-up table based on the bins in Table 1 of paper [30].

The Reindl et al. 1990 model [28] is used to calculate diffuse solar irradiance on horizontal plane $G_{sol;d}$ (W/m^2) as follows:

$$k_T \leq 0.3 \rightarrow G_{sol;d} = (1.020 - 0.148 \cdot k_T) \cdot G_{sol;g}, \tag{7}$$

$$0.3 < k_T < 0.78 \rightarrow G_{sol;d} = (1.45 - 1.67 \cdot k_T) \cdot G_{sol;g}, \tag{8}$$

$$k_T \geq 0.78 \rightarrow G_{sol;d} = 0.147 \cdot G_{sol;g}, \tag{9}$$

The Liu et al. 1960 model [24] is used to calculate direct irradiance on tilted/oriented surface I_{dir} (W/m^2) as follows:

$$I_{dir} = \frac{G_{sol;b}}{\sin \alpha_{sol}} \cdot \cos \theta_{sol;ic}, \tag{10}$$

where

$G_{sol;b}$ is the direct solar irradiance on horizontal plane (W/m^2).

$\theta_{sol;ic}$ is the solar angle of incidence on the inclined surface.

$\frac{G_{sol;b}}{\sin \alpha_{sol}}$ is calculated using the Formula (18) proposed in [17].

The Perez et al. 1990 and the Perez et al. 1990* model [26] are used to calculate diffuse irradiance on tilted/oriented surface I_{dif} (W/m^2) as follows:

$$I_{dif} = G_{sol;d} \cdot \left\{ (1 - F_1) \cdot \frac{[1 + \cos \beta_{ic}]}{2} + F_1 \cdot \frac{a}{b} + F_2 \cdot \sin \beta_{ic} \right\}, \quad (11)$$

where

a, b are dimensionless parameters.

F_1, F_2 is the circumsolar and horizontal brightness coefficient, function of ε.

ε is the dimensionless clearness parameter, at anisotropic sky conditions.

$$\varepsilon = \frac{\left[\frac{G_{sol;d} + G_{sol;b}}{G_{sol;d}} + 1.041 \cdot \left(\frac{\pi \cdot \theta_z}{180} \right)^3 \right]}{1 + 1.041 \cdot \left(\frac{\pi \cdot \theta_z}{180} \right)^3}$$

but in EN ISO 52010 [16] the angle θ_z was replaced by the angle α_{sol} and the coefficient 1.041 was replaced by 1.014

$$\varepsilon^* = \frac{\left[\frac{G_{sol;d} + G_{sol;b}}{G_{sol;d}} + 1.014 \cdot \left(\frac{\pi \cdot \alpha_{sol}}{180} \right)^3 \right]}{1 + 1.014 \cdot \left(\frac{\pi \cdot \alpha_{sol}}{180} \right)^3}$$

3. Case Study

Design choices for the case study are illustrated and justified below, with the aim of showing how the use of different hourly calculation algorithms for the prediction of direct and diffuse solar irradiances on inclined and/or oriented surfaces can vary the outputs of EN ISO 52016-1 [4].

3.1. Locations

The five European locations considered in the case study are: De Bilt (Netherlands), Malaga (Spain), Paris (France), Rome (Italy) and Stockholm (Sweden). As already specified in [17], the choice of cities characterised by very different climates (see Table 2) made it possible to test the performance and limits of the four different calculation algorithms as a function of geographical area. For each city, climate data (TMY) were obtained from weather stations officially recognised by the World Meteorological Organization (WMO).

Table 2. Main climate data of the analysed cities. Gsol,g,H,max: Maximum horizontal global solar irradiance, Cfb: temperate climates with humid summers, Csa: temperate climates with dry summers, Dfb: cold climates with wet winters.

	De Bilt	Malaga	Paris	Rome	Stockholm
Gsol, g, H, max [W/m^2]	896	1038	946	1045	848
Tmax [°C]	32.0	40.2	33.7	36.9	30.5
Tmin [°C]	−7.2	2.1	−4.2	−2.4	−15.3
Climate classification (Köppen/Geiger)	Cfb	Csa	Cfb	Csa	Dfb

3.2. Geometry and Opaque Surfaces

The case study's simplified cube-shaped building has internal dimensions 3.00 m × 3.00 m × 3.00 m. There are no internal partitions and therefore only one air-conditioned thermal zone is considered.

Table 3 shows the geometric characteristics of the building, identifying the net internal area (A_{floor_int}), the external area of the walls for each orientation (A_{wall}), the area of the flat roof (A_{roof_hor}) and the internal volume (V).

Table 3. Geometrical characteristics of building model.

A_{floor_int} [m^2]	9.00
A_{wall} [m^2]	10.22
A_{roof_hor} [m^2]	14.52
V [m^3]	27.00

The thermal transmittance of opaque elements (external walls and flat roof) was determined by considering the thermal transmittances of the individual locations studied, then choosing the average value of approximately 0.50 W/m^2K.

3.3. Transparent Surfaces

Two window types were simulated, one with standard glass and one with low-emissivity glass, in order to assess the impact of this parameter on the final calculation. Both windows have dimensions of 1.20 m × 2.10 m, a thermal transmittance of 1.10 W/m^2K and zero frame area. The window with standard double glazing and argon gas cavity has a solar transmission factor (g_{gl}) of 0.63, while the window with low-emissivity double glazing and argon gas cavity has a g_{gl} of 0.28 (see Table 4).

Table 4. Thermal transmittance and solar transmission coefficient of the windows used.

g_{gl}	b_{window}	h_{window}	U
[-]	[m]	[m]	[W/m^2K]
0.28	1.20	2.10	1.10
0.63	1.20	2.10	1.10

For each window orientation (north, south, east, west, horizontal) a different simulation was performed in order to separate the effects of the direct and diffuse irradiances simulated with the four algorithms on the calculation of the energy demand obtained with EN ISO 52016-1 [4].

3.4. Other Assumptions

Thermal bridges, shading caused by internal or external elements and internal gains were not considered. Ground exchange was considered adiabatic. The ventilation rate was set at 0.50 1/h. The heating and cooling system is assumed on 24 h a day with set-point temperatures of 20 °C and 26 °C, respectively.

To summarise, in this work, one building, two types of glazed surfaces, four different calculation procedures for the prediction of direct and diffuse solar radiation on inclined/oriented surfaces, five locations and five window orientations were considered, for a total of 200 simulations (see Figure 2).

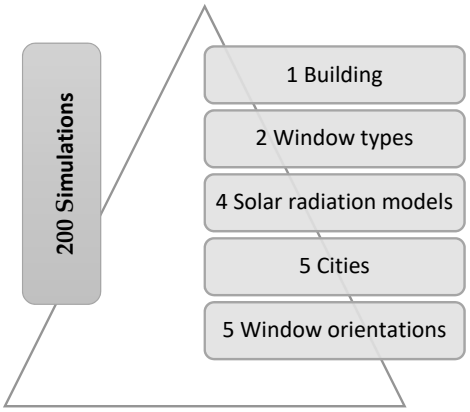

Figure 2. Simulations performed: evaluation of four methods of calculating solar irradiance on a building at variable orientation, position and solar transmission coefficient of windows.

4. Results and Discussions

4.1. Statistical Descriptors

The simulated energy needs for the different cities and with the different solar irradiance data sets were compared using the average, the standard deviation, the mean error and the RMSE (root-Mean-Square Error).

The average of the energy demand value (heating or cooling) for each city is:

$$\overline{x} = \frac{1}{N}\sum_{i=1}^{N} x_i \ \ [\text{kWh/year}],$$

where

x_i: *i*-th annual energy demand value (heating or cooling) determined using as input the set of solar irradiances calculated with the models described in Section 2.

N: number of models used (N = 4).

The standard deviation is used to express the dispersion of the data around the position index, which in our case is the arithmetic mean of the annual energy needs for heating and cooling for each city

$$\sigma = \sqrt{\frac{1}{N}\sum_{i=1}^{N}(x_i - \overline{x})^2} \ [\text{kWh/year}], \quad (12)$$

where

x_i: *i*-th annual energy demand value (heating or cooling) determined using as input the set of solar irradiances calculated with the models described in Section 2.

$\overline{x}$: average value of the annual energy demand (heating or cooling) determined using as input the set of solar irradiances calculated with the models described in Section 2.

N: number of models used (N = 4).

The mean error or uncertainty for each city is:

$$x(\%) = \frac{\sigma}{\overline{x}} \ \ [\%],$$

The RMSE, on the other hand, being proportional to the size of the squared error, is also sensitive to outliers [33,34] and in this case indicates the distance in terms of hourly energy needs of the B-L, E-P* and P-P models compared to the R-P model of TRNSYS.

$$\text{RMSE} = \sqrt{\sum_{i=1}^{n}\frac{(P_i - O_i)^2}{n}} [\text{Wh}], \quad (13)$$

where

P_i: i-th energy need value determined using as input the set of solar irradiances calculated with TRNSYS type 16 (R-P).

O_i: i-th energy need value determined using as input the solar irradiance sets calculated with the B-L, E-P* and P-P models.

n: number of hours when there is an energy need for heating/cooling.

The solar irradiances calculated with TRNSYS Type 16c are taken as benchmark, because this type contains the two split models considered most valid in the literature, namely Reindl [28] and Perez [26]. In addition to Perez's well-known anisotropic sky model, Reindl's model is the only one of those analysed that includes multiple predictor variables in the calculation of direct solar irradiance in the horizontal plane, i.e., the clarity index, solar altitude angle, air temperature and relative humidity. Furthermore, Reindl states that although the clarity index is the most important variable for low or medium clearness index (k_T) values (cloudy sky), in the case of high k_T values (clear sky) the solar altitude angle becomes predominant, improving the irradiance prediction compared to Erbs' model by 26% [28] (model used by EN ISO 52010-1 [16]).

4.2. Impact of Solar Decomposition and Transposition Models on Calculated Energy Demand

The annual energy needs for heating and cooling were compared with the respective solar loads by varying the orientation of the glass surface for the five European locations studied. The solar loads are calculated from the solar irradiances (input data) simulated with the four different calculation models described in Section 2. Each point in Figures 3 and 4 is represented with an abbreviation X_n, where X identifies the orientation of the glazed surface (S: South, E: East, W: West, N: North and H: Horizontal) and n identifies the locations of the case study (1: De Bilt, 2: Malaga, 3: Paris, 4: Rome and 5: Stockholm). Each location is also represented with a different symbol (circle: De Bilt, square: Malaga, rhombus: Paris, triangle: Rome and asterisk: Stockholm) and for each graph there are four identical symbols identifying the four calculation models used for splitting direct and diffuse irradiance on inclined and oriented surfaces (see Section 2).

4.2.1. Case Study with g_{gl} = 0.28

Looking at the case of the g_{gl} = 0.28, it is evident from Figure 3 that the winter solar loads are less dispersed than the summer ones, despite varying location, window orientation and calculation method.

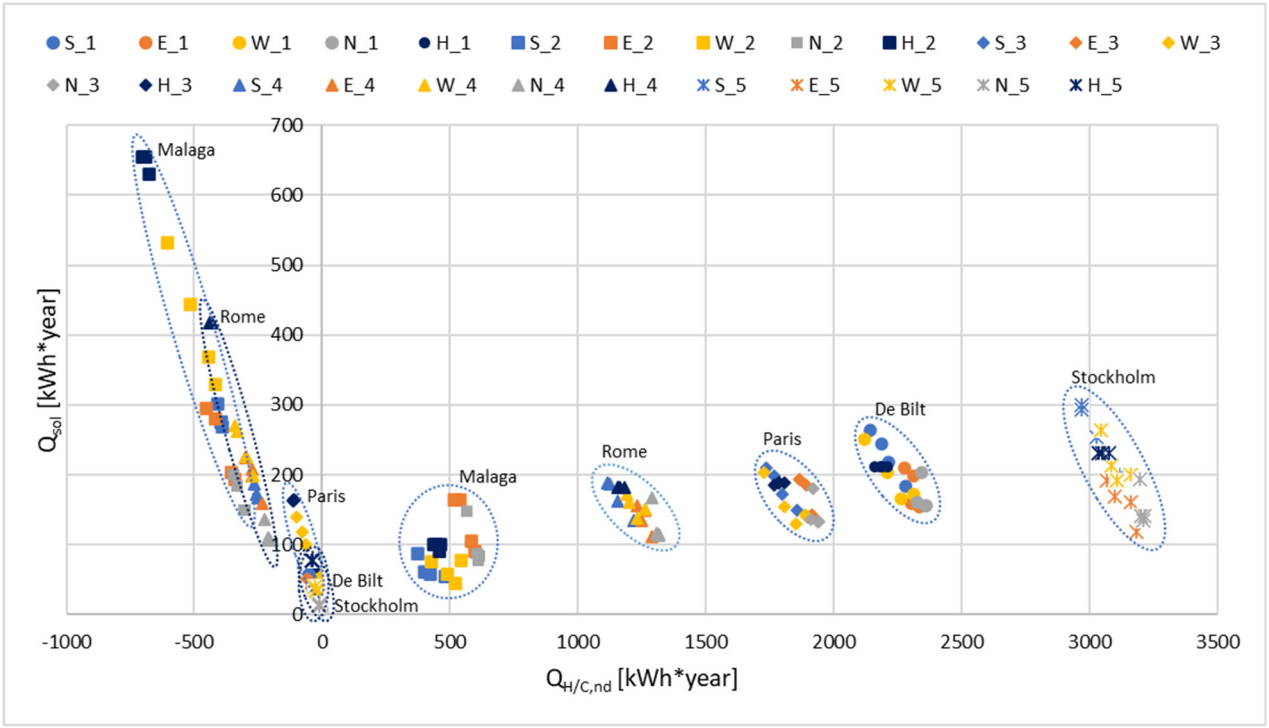

Figure 3. Case g_{gl} = 0.28. Yearly heating (positive) and cooling (negative) energy needs as a function of yearly solar loads calculated from simulated solar irradiances with four different calculation models. Legend: X_n, where X denotes the window orientations (South, East, West, North and Horizontal) and n denotes the locations (1: De Bilt, 2: Malaga, 3: Paris, 4: Rome and 5: Stockholm).

Focusing on the winter period (see Table A1), it can be observed that on buildings with a rooflight (horizontal window placed on the ceiling), the four irradiance calculation models lead to similar standard deviations (henceforth dev.s) for all five locations, both in terms of incoming solar loads (1.2 kWh/year) and in terms of energy needs (16.0 kWh/year). In fact, taking as baseline the hourly heating needs obtained using the solar irradiances calculated with the TRNSYS R-P split method, the RMSEs of the other three models are very low, with values of 6.1 Wh, 6.3 Wh and 9.5 Wh for the B-L, P-P and E-P* methods, respectively (see Table 5).

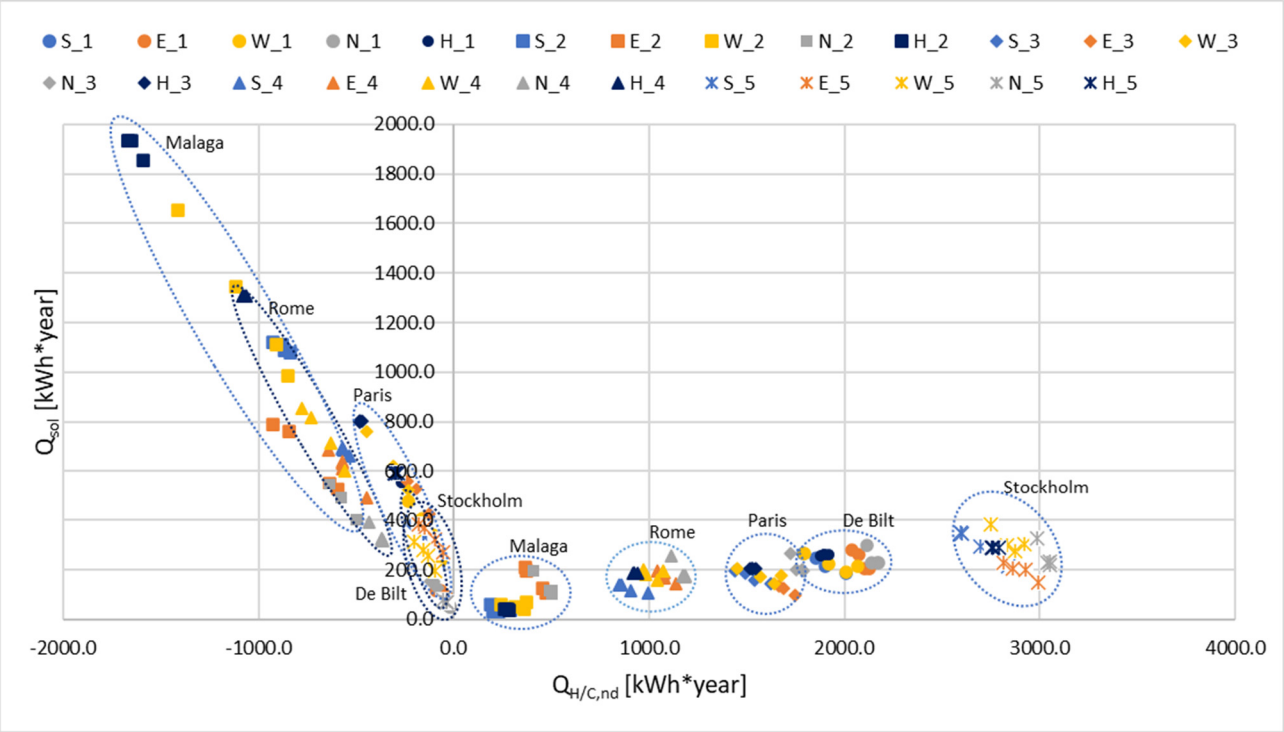

Figure 4. Case g_{gl} = 0.63. Yearly heating (positive) and cooling (negative) energy needs as a function of yearly solar loads calculated from simulated solar irradiances with four different calculation models. Legend: X_n, where X denotes the window orientations (South, East, West, North and Horizontal) and n denotes the locations (1: De Bilt, 2: Malaga, 3: Paris, 4: Rome and 5: Stockholm).

Table 5. Case study with g_{gl} = 0.28. Average RMSE of heating and cooling demand when varying the solar irradiance transposition method. The blue boxes indicate the worst results for heating and the red boxes the worst results for cooling. The asterisk * used beside "E-P*" indicates the change in EN ISO 52010 [16] from the classical method of Perez et al. 1990 on the calculation of the "dimensionless clarity parameter" (see Formula (11)).

	B-L		E-P*		P-P	
	$RMSE_{QH}$	$RMSE_{QC}$	$RMSE_{QH}$	$RMSE_{QC}$	$RMSE_{QH}$	$RMSE_{QC}$
	[Wh]					
Horizontal	6.1	9.2	9.5	14.6	6.3	8.7
South	22.5	21.4	41.0	28.7	20.2	17.5
East	16.3	38.3	23.3	46.9	22.5	55.1
West	27.5	57.5	45.4	106.3	32.9	69.6
North	8.1	22.8	19.3	34.0	9.4	24.6

Remaining still on the winter period of the graph in Figure 3, considering the buildings with south, east, west and north glazed surfaces, the dev.s. of the total solar loads between the different models is similar and equal, respectively, to 29.4 kWh/year, 29.0 kWh/year, 26.6 kWh/year and 26.3 kWh/year, while the dev.s. of the annual heating energy demand is more variable (see Table 6), showing higher values for the south and west orientations with a corresponding average dev.s. among all the cities of the case study of 54.4 kWh/year and 56.8 kWh/year, equal in both cases to about 3.2% on the calculation of the heating energy demand.

Table 6. Case study with g_{gl} = 0.28. Yearly heating and cooling energy demand obtained by averaging the results of the simulated solar irradiance datasets with the four calculation models described in Section 2 and their corresponding standard deviations. The blue boxes indicate the worst results for heating and the red boxes the worst results for cooling.

	Q_H [kWh/Year]								Q_C [kWh/Year]							
	S		E		W		N		S		E		W		N	
	avg	dev.s	avg	dev.s	avg	dev.s	avg	dev.s	avg	dev.s	avg	dev.s	avg	dev.s	avg	dev.s
De Bilt	2205.2	58.6	2306.8	23.3	2226.2	81.2	2347.6	16.2	−8.9	0.8	−7.5	3.1	−17.8	8.5	−4.0	0.7
Malaga	420.1	44.7	559.3	36.3	494.0	50.7	598.8	21.8	−396.7	9.1	−390.6	52.7	−496.0	82.6	−321.5	21.2
Paris	1789.4	51.6	1893.6	20.7	1818.8	70.2	1926.7	14.4	−50.9	1.8	−48.2	9.6	−73.3	21.3	−35.9	2.9
Rome	1153.8	47.3	1259.2	24.2	1222.0	33.2	1307.6	13.7	−256.7	5.0	−271.4	27.0	−308.8	32.9	−212.8	9.4
Stockholm	3020.7	69.9	3127.8	54.3	3099.8	48.5	3207.1	8.4	−18.1	1.8	−18.7	5.6	−21.5	5.2	−9.5	1.1
Average	1717.8	54.4	1829.3	31.7	1772.2	56.8	1877.6	14.9	−146.3	3.7	−147.3	19.6	−183.5	30.1	−116.8	7.1

Focusing on the cities analysed, comparing the dev.s with the average annual winter energy needs estimated with the EN ISO 52016-1 [4] standard when varying the radiation splitting methods, an average error on the energy needs estimate of less than 5% is obtained for all locations, except for Malaga, where the average error is 6.7% and the maximum error 10.6% (south).

Analysing the hourly heating energy needs, it is noted that for all four orientations, the highest RMSE values are those obtained using as input the irradiances calculated with the E-P* method of EN ISO 52010 [16] with values of 41.0 Wh, 23.3 Wh, 45.4 Wh and 19.3 Wh, respectively, for the south, east, west and north orientation (see Table 5). On the other hand, the RMSE values of the B-L and P-P methods were similar and lower than the E-P* method of 47.9%, 16.7%, 33.6% and 54.8% for the south, east, west and north orientation, respectively.

Analysing the summer period (see Figure 3 and Table A1), unlike the winter period, the points appear to be more scattered. The dev.s of the total solar loads for the buildings with south, east, west and north glazed surfaces is 5.6 kWh/year, 18.6 kWh/year, 33.6 kWh/year and 8.7 kWh/year, respectively, while the average dev.s of the annual cooling energy demand (see Table 6) shows higher values mainly for the west orientation with average dev.s values of 30.1 kWh/year, which is 16.4% error in the calculation of the cooling energy demand.

Focusing on the analysed cities, comparing the dev.s with the average annual cooling energy requirements estimated with EN ISO 52016-1 [4], varying the radiation split methods produces an error on the energy requirement estimate significantly higher than 5% for all locations in the case study. In particular, the worst estimate occurs for the De Bilt location where the average error is 23.8% and the maximum error is 47.8% for the west orientation. These high percentages are undoubtedly the result of very low cooling energy demands due to both the location and the low emissivity of the glass; but also for Malaga, where the energy demand is higher, the average error is 8.2% and the maximum error is 16.7% for the western orientation.

Looking from annual to hourly cooling demand, once again the E-P* method appears to be the one with the highest RMSE for the south, west and north orientations with values of 28.9 Wh, 106.3 Wh and 34.0 Wh, respectively; while for the east orientation, the method with the highest RMSE appears to be the P-P with a value of 55.1 Wh (see Table 5).

The methods showing better RMSE, on the other hand, are the B-L for east, west and north orientation with values 30.4%, 46.0% and 33.0% lower than the maximum values, and the P-P method for south orientation with an RMSE 39.3% lower than the maximum values.

To conclude, calculating the maximum delta of heating and cooling requirements for each orientation of the glazed surface and for each location studied (Table 7), varying the irradiance split method leads to annual energy variations of up to 188. 8 kWh/year (21.0 kWh/year/m^2) for heating and up to 184.3 kWh/year (20.5 kWh/year/m^2) for cooling, i.e., a variation of +8.5% and −37.2% compared to the average of the energy needs obtained with the four irradiance split methods.

Table 7. Case study g_{gl} = 0.28. Maximum variation of heating and cooling requirements calculated with the different irradiance sets obtained from the four solar radiation split methods. $\Delta Q_{H/C,max} = Q_{H/C,max,i} - Q_{H/C,min,i}$. The grey cells indicate the highest deltas.

	$\Delta Q_{H,max}$ [kWh/Year]					$\Delta Q_{C,max}$ [kWh/Year]				
	S	**E**	**W**	**N**	**H**	**S**	**E**	**W**	**N**	**H**
De Bilt	139.6	56.0	188.8	36.6	49.2	1.8	7.0	19.8	1.3	3.5
Malaga	105.0	77.7	116.4	47.0	26.6	21.4	112.0	184.3	42.8	27.7
Paris	120.9	50.0	163.3	28.3	38.8	4.0	20.4	49.1	5.3	5.7
Rome	103.4	56.8	72.0	29.7	27.0	11.5	65.5	71.4	20.8	11.0
Stockholm	149.0	116.4	116.3	17.6	42.6	3.5	12.3	12.7	2.5	4.2

4.2.2. Caso Study with g_{gl} = 0.63

By decreasing the window performance and switching from a low-e double glazing unit with g_{gl} of 0.28 to a float double glazing unit with g_{gl} of 0.63 (see Figure 4), the dev.s. between the models analysed increases for both heating and cooling requirements, except for the heating requirements for buildings with horizontal glazing surfaces, where the dev.s. between the models is lower by 2.4 kWh/year (see Table A2).

In the heating season (Table 8), for buildings with south, east, west and north glazed surfaces, the dev.s of solar loads increases compared to the case study with g_{gl} = 0.28, with average values of 30.3 kWh/year (+3.3%), 35.3 kWh/year (+21.7%), 26.7 kWh/year (+0.3%) and 41.2 kWh/year (+54.4%). As a consequence, the dev.s of energy needs also increases compared to the case study with g_{gl} = 0.28, with values of 78.9 kWh/year (+45.0%), 49.8 kWh/year (+56.8%), 80.2 kWh/year (41.2%) and 33.7 kWh/year (+126.4%) for the south, east, west and north orientations, respectively.

Table 8. Case study with g_{gl} = 0.63. Yearly heating and cooling energy demand obtained by averaging the results of the simulated solar irradiance datasets with the four calculation models described in Section 2 and their respective standard deviations. The blue boxes indicate the worst results for heating and the red boxes the worst results for cooling.

	Q_H [kWh/Year]								Q_C [kWh/Year]							
	S		**E**		**W**		**N**		**S**		**E**		**W**		**N**	
	avg	**dev.s**	**avg**	**dev.s**	**avg**	**dev.s**	**avg**	**dev.s**	**avg**	**dev.s**	**avg**	**dev.s**	**avg**	**dev.s**	**avg**	**dev.s**
De Bilt	1888.6	92.0	2086.0	37.7	1947.4	117.9	2147.7	26.9	−88.3	11.0	−59.2	26.4	−143.2	72.0	−26.1	7.1
Malaga	226.0	44.2	416.8	55.6	321.5	60.9	476.2	46.4	−876.3	37.7	−749.8	159.5	−1072.3	255.3	−551.3	67.2
Paris	1523.2	76.3	1707.6	38.3	1584.6	101.0	1762.4	29.0	−197.7	12.5	−171.0	53.5	−294.0	116.3	−97.3	17.0
Rome	900.7	67.6	1082.8	38.7	1016.2	47.5	1162.4	35.1	−561.5	16.7	−557.9	81.9	−675.7	97.5	−383.4	33.6
Stockholm	2682.0	114.4	2901.0	78.5	2843.0	73.6	3032.2	31.2	−138.4	20.8	−120.8	54.4	−147.1	44.5	−41.6	9.4
Average	1444.1	78.9	1638.8	49.8	1542.5	80.2	1716.2	33.7	−372.5	19.7	−331.7	75.1	−466.5	117.1	−219.9	26.9

As in the case of g_{gl} = 0.28, it is evident from Table 8 that the south and west orientations show the highest average dev.s with errors of 5.5% (78.9 kWh/year) and 5.2% (80.2 kWh/year) on the calculation of the heating energy needs, respectively.

Focusing on the cities analysed, comparing the dev.s with the average annual winter demand estimated with EN ISO 52016-1 [4] when varying the solar radiation split methods, the average error among all orientations on the winter demand estimate is less than 5% for all locations except for Malaga, where the average error is 13.9% and the maximum error is 19.6% (south). Different from the case with g_{gl} = 0.28, where all cities showed an error on all orientations of less than 5%, in the case with g_{gl} = 0.63, De Bilt and Paris show an error on the annual demand estimate of 6.1% and 6.4% in the west, while Rome shows an error of 7.5% in the south.

Analysing, instead, the hourly heating energy needs, it can be seen that for all five orientations, the highest RMSE values are those obtained using as input the irradiances calculated with the E-P* method of EN ISO 52010-1 [16] with values of 11.6 Wh, 76.1 Wh, 41.0 Wh, 76.0 Wh and 37.3 Wh, respectively, for the horizontal, south, east, west and north window orientation (see Table 9). The methods that show better RMSE, on the other hand,

are the B-L for the horizontal, east, west and north orientation with values lower than the maximum ones of the E-P* method of 24.0%, 34.0%, 35.7% and 64.2%, and the P-P method for the south orientation with lower RMSE than the maximum of 51.3%.

Table 9. Case study with g_{gl} = 0.63. Average RMSE of heating and cooling demand when varying the solar irradiance transposition method. The blue boxes indicate the worst results for heating and the red boxes the worst results for cooling.

	B-L		E-P*		P-P	
	$RMSE_{QH}$	$RMSE_{QC}$	$RMSE_{QH}$	$RMSE_{QC}$	$RMSE_{QH}$	$RMSE_{QC}$
	[Wh]					
Horizontal	8.8	14.2	11.6	19.2	9.2	14.0
South	43.6	58.1	76.1	86.4	37.0	42.0
East	27.1	89.0	41.0	114.0	37.7	132.9
West	48.9	139.4	76.0	241.9	57.6	166.8
North	13.3	48.0	37.3	79.5	16.6	52.9

In the summer season (see Figure 4 and Table A2), the dev.s of the total solar loads for buildings with south, east, west and north windows is 15.6 kWh/year, 73.4 kWh/year, 142.9 kWh/year and 26.3 kWh/year, respectively, while the average dev.s of the annual cooling energy demand for buildings with south, east, west and north windows (see Table 9) results to be 19.7 kWh/year, 75.1 kWh/year, 117.1 kWh/year and 26.9 kWh/year with an average increase over the case study of g_{gl} = 0.28 of 434.9%, 283.6%, 289.0% and 281.1%.

Furthermore, focusing on the summer period, the variation in the decomposition and transposition models imply a variation on the cooling energy needs substantially greater than 5% for each city. In particular, the worst estimate is for the De Bilt location where the average error is 27.3% and the maximum error is 50.3% for the west orientation. These high percentages are undoubtedly due to very low cooling energy demands, but even for Malaga where the energy demand is higher, the average error is 12.7% and the maximum error is 23.8% for the western orientation.

Regarding the cooling hourly energy needs, the highest RMSEs are given again by the E-P* method with values of 19.2 Wh, 86.4 Wh, 241.9 Wh and 79.5 Wh, respectively, for the horizontal, south, west and north window orientation, while for the east orientation, the worst RMSE value is given by the P-P method equivalent to 132.9 Wh (see Table 8). The best RMSEs are obtained from the P-P models for the horizontal and southern orientation of the glazed surface, with values 27.1% and 51.4% lower than the maximum values of the E-P* method; while the B-L model gives lower RMSEs of 33.1%, 42.4% and 39.6% for the east, west and north orientations.

Calculating the maximum delta of heating and cooling demand for each orientation of the glazing surface and for each location (Table 10), varying the irradiance split method leads to annual energy variations up to 270.2 kWh/year for heating and up to 565.2 kWh/year for cooling, representing a variation of 13.9% and −52.7% compared to the average demand obtained with the four irradiance split methods.

Table 10. Case study g_{gl} = 0.63. Maximum variation of heating and cooling requirements calculated with the different irradiance sets obtained from the four solar radiation split methods. $\Delta Q_{H/C,max} = Q_{H/C,max,i} - Q_{H/C,min,i}$. The grey cells indicate the highest deltas.

	$\Delta Q_{H,max}$ [kWh/Year]					$\Delta Q_{C,max}$ [kWh/Year]				
	S	E	W	N	H	S	E	W	N	H
De Bilt	217.9	88.0	270.2	58.1	39.6	21.4	57.8	166.0	15.3	11.8
Malaga	100.3	109.6	134.4	96.5	25.5	90.9	329.2	565.2	139.8	75.1
Paris	178.9	82.9	231.0	62.5	30.1	26.2	110.7	266.4	35.0	11.2
Rome	148.8	92.2	101.2	73.1	23.3	35.6	197.3	217.8	70.9	15.1
Stockholm	246.0	179.6	173.8	66.6	36.8	37.0	121.4	106.1	19.3	13.2

These results appear to be congruent with Michalak's study [18] where the use of EN ISO 52010-1 for the calculation of solar irradiance leads to a significant change in the energy performance indicator for heating and domestic hot water (EP_{H+W}) compared to that provided in the Polish TMYs, impacting the energy classification of a building. This result is shown to be very important because the improvement of the building's energy class is derived only from the choice of the calculation method of decomposition and transposition of solar irradiance and not from a real efficiency intervention.

5. Conclusions

Defining the boundary conditions of the conditioned environment, such as climate data, is crucial when assessing the energy performance of buildings. Most of these data (such as temperature, humidity and horizontal global irradiance) are available in special databases, while others, such as direct and diffuse solar irradiances on horizontal and inclined/oriented planes, must be estimated with special models obtained from regressions of experimental data gathered in different parts of the world, therefore not perfectly adequate to provide irradiances on every point of the earth's surface. In this study we evaluated four pairs of models for calculating the direct and diffuse irradiance of horizontal and inclined/oriented surfaces (see Section 2) and calculated the uncertainty that these models introduce in the estimation of the energy needs of a building, simulated with the simplified hourly dynamic method of EN ISO 52016-1 [4] on five European locations, also varying the solar transmission coefficient of the glazed surface (g_{gl}). The main results follow:

The dev. of solar loads for the winter period on the various orientations and as the solar transmittance coefficient of glass changes does not cause an excessive increase in incoming solar loads, since winter solar radiation is generally low. For the summer period, on the other hand, the increase in the solar transmittance coefficient of the glass causes a significant increase in incoming solar loads on all orientations with values exceeding 178%.

- The dev.s of the heating energy demands on the various orientations and for both case studies (ggl), show average values of uncertainty on the calculation of the total energy demand for heating below or slightly above 5%, thus acceptable.
- On the other hand, when calculating the cooling demand, in both case studies, the largest errors are obtained for the west orientation of the glazed area, with average uncertainty values on the calculation of the total energy demand for cooling of 16.4 percent. In contrast to the heating needs, considering also the other orientations, the average errors on the estimation of the cooling demand are considerably higher than 5% and therefore not acceptable.
- Focusing on the individual localities, while the estimation of the annual winter demand by varying the solar radiation split methods shows an average error of less than 5%, the individual city of Malaga shows errors on the winter demand estimation up to 10.6% with g_{gl} = 0.28 and up to 19.6% with g_{gl} = 0.63. This indicates that some of the split methods used are less appropriate to predict irradiance for the city of Malaga.
- On the other hand, comparing the dev.s with the respective average annual summer demand when varying the radiation split methods, an error on the estimation of the energy demand that is 5% higher for all locations is obtained for both the case study with g_{gl} = 0.28 and with g_{gl} = 0.63. This indicates that the solar radiation split methods for estimating cooling requirements severely affect the results of EN ISO 52016-1 [4], especially for De Bilt where the average error considering all orientations is 27.3%.
- Calculating the RMSE of both hourly heating and cooling needs and taking as baseline the results obtained using the R-P solar radiation split method contained in TRNSYS, for both g_{gl} = 0.28 and g_{gl} = 0.63, the model that deviates the most from these results is the one contained in EN ISO 52010-1 [16], i.e., the E-P* model.

Possible future developments will be to compare models of solar irradiance splitting the components on inclined and oriented surfaces with real data collected experimentally with pyranometers placed vertically on each main orientation. Furthermore, the experi-

mentally measured solar loads will be compared with the solar loads identified with the main simulation software.

Author Contributions: Conceptualization, S.S.; methodology, S.S.; software, G.R.; validation, S.S.; formal analysis, S.S. and G.R.; investigation, S.S.; resources, S.S.; data curation, S.S. and G.R.; writing—original draft preparation, S.S.; writing—review and editing, S.S.; visualization, S.S. and G.R.; supervision, G.C. and C.D.P.; project administration, C.D.P.; Funding acquisition, A.S. All authors have read and agreed to the published version of the manuscript.

Funding: This research received no external funding.

Data Availability Statement: The data presented in this study are available on request from the corresponding author. The data are not publicly available due to data from licensed software.

Conflicts of Interest: The authors declare no conflict of interest.

Appendix A

Table A1. Case study ggl = 0.28. Heating/cooling energy demand and solar loads obtained using the four different solar irradiance decomposition and transposition models. The asterisk * used beside "E-P*" indicates the change in EN ISO 52010 [16] from the classical method of Perez et al. 1990 on the calculation of the "dimensionless clarity parameter" (see Formula (11)).

			S		E		W		N		H	
			Q_{nd}	Q_{sol}	Q_{nd}	Q_{sol}	Q_{nd}	Q_{sol}	Q_{nd}	Q_{sol}	Q_{nd}	Q_{sol}
			kWh									
De Bilt	Heating	B-L	2214.0	217.0	2332.4	153.3	2207.6	201.0	2357.1	154.5	2182.5	210.2
		E-P*	2280.6	182.6	2313.8	196.4	2310.9	170.4	2343.4	201.0	2211.4	210.2
		P-P	2185.1	241.9	2276.4	208.1	2264.0	163.9	2363.3	153.8	2185.5	210.2
		R-P	2141.0	262.9	2304.4	157.0	2122.1	249.4	2326.7	158.5	2162.2	209.2
	Cooling	B-L	−7.8	16.9	−4.6	9.8	−19.3	47.1	−3.5	5.9	−31.5	65.3
		E-P*	−9.1	18.6	−7.9	12.9	−9.1	27.3	−4.5	6.1	−29.7	65.3
		P-P	−9.1	18.5	−11.7	12.6	−13.8	39.6	−3.4	5.2	−31.5	65.3
		R-P	−9.6	17.6	−5.7	10.1	−28.9	55.8	−4.6	6.5	−33.2	65.2
Malaga	Heating	B-L	423.1	55.7	583.3	102.8	488.8	56.1	613.6	83.0	444.6	98.3
		E-P*	480.3	53.5	540.8	161.6	541.7	75.0	566.5	145.7	462.6	98.3
		P-P	375.3	84.8	517.6	162.8	520.3	42.6	609.5	76.5	436.0	98.3
		R-P	401.6	60.2	595.3	89.4	425.3	74.0	605.4	86.2	457.7	89.5
	Cooling	B-L	−388.3	266.6	−354.5	202.4	−516.4	441.6	−305.3	147.3	−704.1	653.0
		E-P*	−409.7	300.1	−417.1	278.7	−419.1	327.3	−344.6	198.0	−689.1	653.0
		P-P	−394.6	273.8	−451.4	292.9	−445.1	366.1	−301.8	148.1	−700.6	653.0
		R-P	−394.1	274.2	−339.4	192.3	−603.4	531.2	−334.5	181.8	−676.4	627.8
Paris	Heating	B-L	1799.4	170.5	1916.1	140.8	1809.6	153.3	1937.8	131.2	1784.3	186.3
		E-P*	1856.1	147.7	1894.5	183.8	1888.6	141.5	1916.9	179.5	1806.7	186.3
		P-P	1766.8	196.5	1866.1	192.3	1851.8	128.3	1940.2	130.7	1784.6	186.3
		R-P	1735.1	208.6	1897.8	138.2	1725.3	201.2	1911.8	135.2	1767.9	183.7
	Cooling	B-L	−48.4	53.5	−40.3	37.0	−77.3	117.3	−33.6	27.2	−111.4	162.6
		E-P*	−51.9	59.4	−50.6	48.7	−52.0	76.0	−38.5	32.2	−107.1	162.6
		P-P	−50.7	57.0	−60.7	49.9	−62.6	99.2	−33.1	26.2	−111.0	162.6
		R-P	−52.5	55.6	−41.2	37.1	−101.1	138.6	−38.3	31.4	−112.9	161.6

Table A1. *Cont.*

			S		E		W		N		H	
			Q_{nd}	Q_{sol}	Q_{nd}	Q_{sol}	Q_{nd}	Q_{sol}	Q_{nd}	Q_{sol}	Q_{nd}	Q_{sol}
			kWh									
Rome	Heating	B-L	1157.3	160.1	1290.2	109.4	1191.9	170.0	1317.9	114.1	1162.0	179.9
		E-P*	1219.3	133.1	1264.1	147.7	1263.8	148.7	1288.1	164.9	1181.9	179.9
		P-P	1122.7	184.6	1233.3	154.4	1233.3	135.8	1316.5	112.4	1159.4	179.9
		R-P	1116.0	186.7	1249.3	133.2	1199.0	159.2	1307.8	115.8	1154.9	179.9
	Cooling	B-L	−251.8	165.5	−235.8	157.9	−340.7	269.1	−208.4	107.4	−439.5	415.8
		E-P*	−263.3	185.7	−273.4	206.4	−269.2	196.0	−226.6	134.1	−428.5	415.8
		P-P	−254.3	170.8	−301.4	223.5	−294.6	225.0	−205.8	105.7	−436.5	415.8
		R-P	−257.4	171.3	−275.0	196.2	−330.5	260.9	−210.4	109.1	−439.3	415.8
Stockholm	Heating	B-L	3029.0	252.8	3183.4	115.9	3043.5	262.0	3216.4	138.9	3047.2	228.9
		E-P*	3116.4	199.2	3162.3	158.6	3159.8	198.4	3198.8	191.1	3078.2	228.9
		P-P	2967.4	298.0	3098.5	166.6	3086.3	211.3	3211.9	132.4	3037.8	228.9
		R-P	2969.9	292.0	3067.0	189.7	3109.5	190.6	3201.5	139.8	3035.7	228.9
	Cooling	B-L	−16.4	26.8	−12.0	24.8	−28.1	38.3	−8.6	11.0	−38.6	75.8
		E-P*	−16.8	28.0	−16.0	30.8	−15.4	24.9	−11.0	13.6	−35.9	75.8
		P-P	−19.3	29.5	−22.3	34.9	−22.0	33.4	−8.9	10.8	−39.3	75.8
		R-P	−20.0	29.6	−24.3	36.2	−20.6	31.9	−9.6	11.2	−40.1	75.8

Table A2. Case study ggl = 0.63. Heating/cooling energy demand and solar loads obtained using the four different solar irradiance decomposition and transposition models. The asterisk * used beside "E-P*" indicates the change in EN ISO 52010 [16] from the classical method of Perez et al. 1990 on the calculation of the "dimensionless clarity parameter" (see Formula (11)).

			S		E		W		N		H	
			Q_{nd}	Q_{sol}	Q_{nd}	Q_{sol}	Q_{nd}	Q_{sol}	Q_{nd}	Q_{sol}	Q_{nd}	Q_{sol}
			kWh									
De Bilt	Heating	B-L	1903.1	209.5	2128.0	201.1	1918.5	220.8	2165.9	222.4	1893.8	255.3
		E-P*	2007.9	182.3	2074.4	254.9	2066.1	209.7	2115.3	294.0	1917.3	255.3
		P-P	1853.6	244.5	2040.0	274.5	2009.1	185.3	2173.4	223.1	1895.4	255.3
		R-P	1790.0	261.7	2101.4	200.3	1795.9	262.0	2136.2	222.3	1877.6	253.4
	Cooling	B-L	−76.8	214.3	−35.7	86.3	−161.2	399.2	−21.0	48.0	−262.1	553.1
		E-P*	−81.0	216.4	−66.2	111.6	−69.1	231.8	−35.5	53.9	−255.2	553.1
		P-P	−98.2	236.0	−93.5	112.0	−107.5	335.1	−20.1	44.6	−261.1	553.1
		R-P	−97.3	228.3	−41.3	88.0	−235.1	473.7	−27.7	53.8	−267.0	552.7
Malaga	Heating	B-L	226.7	28.2	453.2	119.9	312.5	48.0	501.7	109.5	264.7	35.9
		E-P*	287.7	31.1	372.8	192.8	373.4	64.7	407.0	192.6	278.1	35.9
		P-P	187.3	56.1	365.8	204.0	360.9	35.3	503.6	99.0	257.9	35.9
		R-P	202.2	27.2	475.4	102.4	239.0	54.0	492.4	110.0	283.4	34.2
	Cooling	B-L	−835.5	1073.4	−633.9	547.2	−1117.3	1341.9	−498.8	395.2	−1668.6	1927.1
		E-P*	−866.9	1085.5	−841.3	758.5	−848.9	978.6	−634.4	541.6	−1649.1	1927.1
		P-P	−926.4	1117.1	−926.6	785.5	−909.0	1106.6	−494.6	395.4	−1666.4	1927.1
		R-P	−876.6	1106.1	−597.4	521.5	−1414.1	1648.1	−577.3	484.1	−1593.6	1850.9

Table A2. *Cont.*

			S		E		W		N		H	
			Q_{nd}	Q_{sol}	Q_{nd}	Q_{sol}	Q_{nd}	Q_{sol}	Q_{nd}	Q_{sol}	Q_{nd}	Q_{sol}
			kWh									
Paris	Heating	B-L	1539.1	152.6	1745.7	93.1	1571.9	165.9	1782.9	196.0	1527.4	202.4
		E-P*	1621.0	138.5	1689.5	122.5	1679.4	170.5	1724.0	262.7	1545.6	202.4
		P-P	1490.5	181.5	1662.8	130.6	1638.6	142.0	1786.5	193.2	1527.1	202.4
		R-P	1442.1	189.2	1732.4	161.3	1448.4	200.4	1756.1	196.6	1515.5	199.4
	Cooling	B-L	−181.6	357.3	−127.6	418.7	−311.6	618.1	−83.8	127.2	−481.6	797.9
		E-P*	−194.2	366.5	−189.5	522.9	−182.9	391.8	−117.8	149.2	−471.9	797.9
		P-P	−207.3	383.4	−238.3	556.2	−232.2	517.2	−82.8	121.1	−480.0	797.9
		R-P	−207.8	373.8	−128.4	607.6	−449.3	757.3	−104.8	148.9	−483.1	793.8
Rome	Heating	B-L	904.1	112.2	1136.7	137.9	970.1	193.5	1183.5	174.1	923.0	182.2
		E-P*	994.8	101.8	1073.4	188.1	1071.3	191.8	1110.4	251.1	940.2	182.2
		P-P	857.6	136.0	1044.5	192.8	1039.6	153.7	1183.4	168.4	920.8	182.2
		R-P	846.1	133.6	1076.5	161.3	983.7	177.8	1172.1	173.7	916.8	182.2
	Cooling	B-L	−537.0	657.2	−446.5	486.1	−779.1	850.7	−366.6	317.2	−1078.6	1300.8
		E-P*	−565.2	682.5	−572.3	633.3	−561.3	599.4	−433.5	386.6	−1063.7	1300.8
		P-P	−571.3	688.9	−643.8	679.4	−632.8	710.5	−362.7	313.6	−1075.4	1300.8
		R-P	−572.6	688.4	−569.2	607.6	−729.6	810.4	−370.7	320.9	−1078.8	1300.8
Stockholm	Heating	B-L	2694.4	287.5	2995.5	142.8	2747.8	377.6	3051.4	228.2	2763.0	285.6
		E-P*	2839.2	211.2	2930.2	196.8	2921.6	296.9	2986.5	322.0	2790.2	285.6
		P-P	2593.2	344.7	2862.6	200.9	2830.6	294.7	3053.1	214.0	2754.3	285.6
		R-P	2601.4	338.9	2815.8	223.6	2872.1	270.0	3037.8	225.3	2753.4	285.6
	Cooling	B-L	−120.3	302.1	−56.3	263.6	−204.5	309.2	−36.6	65.1	−297.0	587.3
		E-P*	−120.5	304.1	−97.6	318.1	−98.4	189.1	−55.7	76.0	−288.4	587.3
		P-P	−155.4	339.9	−151.7	364.7	−153.6	274.5	−36.4	64.1	−299.2	587.3
		R-P	−157.3	342.5	−177.7	380.1	−131.8	252.6	−37.6	63.7	−301.6	587.3

References

1. International Energy Agency (IEA). Net Zero by 2050. Available online: https://www.iea.org/reports/net-zero-by-2050 (accessed on 28 September 2022).
2. European Commission. Energy Performance of Buildings Directive, An Official Website of the European Union. 2021. Available online: https://energy.ec.europa.eu/topics/energy-efficiency/energy-efficient-buildings/energy-performance-buildings-directive_en (accessed on 28 September 2022).
3. Van Dijk, D.; Hogeling, J. The new EN ISO 52000 family of standards to assess the energy performance of buildings put in practice. *REHVA J.* **2019**, *111*, 04047. [CrossRef]
4. *EN ISO 52016-1:2017*; Energy Performance of Buildings—Energy Needs for Heating and Cooling, Internal Temperatures and Sensible and Latent Head Loads—Part 1: Calculation Procedures Performance. European Committee for Standardization: Brussels, Belgium, 2017.
5. van Dijk, D. EPB standards: Why choose hourly calculation procedures? Federation of European Heating, Ventilation and Air Conditioning Associations: 40 Rue Washington 1050 Brussels, Belgium. *REHVA J.* **2018**, *2*, 6–12. Available online: https://www.rehva.eu/rehva-journal/chapter/epb-standards-why-choose-hourly-calculation-procedures (accessed on 28 September 2022).
6. Ballarini, I.; Costantino, A.; Fabrizio, E.; Corrado, V. A Methodology to Investigate the Deviations between Simple and Detailed Dynamic Methods for the Building Energy Performance Assessment. *Energies* **2020**, *13*, 6217. [CrossRef]
7. Zakula, T.; Badun, N.; Ferdelji, N.; Ugrina, I. Framework for the ISO 52016 standard accuracy prediction based on the in-depth sensitivity analysis. *Appl. Energy* **2021**, *298*, 117089. [CrossRef]
8. Mazzarella, L.; Scoccia, R.; Colombo, P.; Motta, M. Improvement to EN ISO 52016-1:2017 hourly heat transfer through a wall assessment: The Italian National Annex. *Energy Build.* **2020**, *210*, 109758. [CrossRef]
9. Summa, S.; Remia, G.; Di Perna, C. Comparative and Sensitivity Analysis of Numerical Methods for the Discretization of Opaque Structures and Parameters of Glass Components for EN ISO 52016-1. *Energies* **2022**, *15*, 1030. [CrossRef]
10. De Luca, G.; Bianco Mauthe Degerfeld, F.; Ballarini, I.; Corrado, V. Improvements of simplified hourly models for the energy assessment of buildings: The application of EN ISO 52016 in Italy. *Energy Reports* **2022**, *8*, 7349–7359. [CrossRef]
11. Magni, M.; Ochs, F.; Streicher, W. Comprehensive analysis of the influence of different building modelling approaches on the results and computational time using a cross-compared model as a reference. *Energy Build.* **2022**, *259*, 111859. [CrossRef]

12. Radhi, H. A comparison of the accuracy of building energy analysis in Bahrain using data from different weather periods. *Renew. Energy* **2009**, *34*, 869–875. [CrossRef]
13. Taylor, J.; Davies, M.; Mavrogianni, A.; Chalabi, Z.; Biddulph, P.; Oikonomou, E.; Das, P.; Jones, B. The relative importance of input weather data for indoor overheating risk assessment in dwellings. *Build. Environ.* **2014**, *76*, 81–91. [CrossRef]
14. Li, H.; Yang, Y.; Lv, K.; Liu, J.; Yang, L. Compare several methods of select typical meteorological year for building energy simulation in China. *Energy* **2020**, *209*, 118465. [CrossRef]
15. Plokker, W.; van Dijk, D. *EPB Standard EN ISO 52010*; Conversion of Climatic Data for Energy Calculations: Completion of A Missing Link. REHVA Federation of European Heating, Ventilation and Air Conditioning Associations: Brussels, Belgium, 2016. Available online: https://www.rehva.eu/rehva-journal/chapter/epb-standard-en-iso-52010-conversion-of-climatic-data-for-energy-calculations-completion-of-a-missing-link (accessed on 28 September 2022).
16. *ISO 52010-1:2017*; Energy Performance of Buildings—External Climatic Conditions—Part 1: Conversion of Climatic Data for Energy Calculations. International Organization for Standardization: Geneva, Switzerland, 2017. Available online: https://www.iso.org/standard/65703.html (accessed on 28 September 2022).
17. Summa, S.; Tarabelli, L.; Di Perna, C. Evaluation of ISO 52010-1: 2017 and proposal for an alternative calculation procedure. *Sol. Energy* **2021**, *218*, 262–281. [CrossRef]
18. Michalak, P. Modelling of Solar Irradiance Incident on Building Envelopes in Polish Climatic Conditions: The Impact on Energy Performance Indicators of Residential Buildings. *Energies* **2021**, *14*, 4371. [CrossRef]
19. *EN ISO 13790: 2008*; Energy Performance of Buildings—Calculation of Energy Use for Space Heating and Cooling CEN. European Commitee for Standardization: Brussels, Belgium, 2008.
20. *UNI 10349-1:2016*; Riscaldamento E Raffrescamento Degli Edifici—Dati Climatici—Parte 1: Medie Mensili per la Valutazione Della Prestazione Termo-Energetica Dell'Edificio E Metodi per Ripartire L'Irradianza Solare Nella Frazione Diretta E Diffusa E per C. UNI—Ente Italiano di Normazione: Milan, Italy, 2016.
21. *Meteonorm 7*, Version 7.3.3; Meteotest: Bern, Switzerland, 2018. Available online: https://meteonorm.com/en/2018(accessed on 28 September 2022).
22. Duffy, M.J.; Hiller, M.; Bradley, D.E.; Werner Keilholz, J.W. *TRNSYS 17: A Transient System Simulation Program, 2010*; Solar Energy Laboratory, University of Wisconsin: Madison, WI, USA, 2013. Available online: https://sel.me.wisc.edu/trnsys/features/features.html (accessed on 28 September 2022).
23. Boland, J.; Ridley, B.; Brown, B. Models of diffuse solar radiation. *Renew. Energy* **2008**, *33*, 575–584. [CrossRef]
24. Liu, B.Y.H.; Jordan, R.C. The interrelationship and characteristic distribution of direct, diffuse and total solar radiation. *Sol. Energy* **1960**, *4*, 1–19. [CrossRef]
25. Erbs, D.G.; Klein, S.A.; Duffie, J.A. Estimation of the diffuse radiation fraction for hourly, daily and monthly-average global radiation. *Sol. Energy* **1982**, *28*, 293–302. [CrossRef]
26. Perez, R.; Ineichen, P.; Seals, R.; Michalsky, J.; Stewart, R. Modeling daylight availability and irradiance components from direct and global irradiance. *Sol. Energy* **1990**, *44*, 271–289. [CrossRef]
27. Perez, R.; Ineichen, P.; Maxwell, E.; Seals, R.; Zelenka, A. Dynamic Models for hourly global-to-direct irradiance conversion. In Proceedings of the Solar World Congress, Denver, CO, USA, 19–23 August 1991.
28. Reindl, D.T.; Beckman, W.A.; Duffie, J.A. Diffuse fraction correlations. *Sol. Energy* **1990**, *45*, 1–7. [CrossRef]
29. Maxwell, E.L. *A Quasi-Physical Model for Converting Hourly Global Horizontal to Direct Normal Insolation*; Solar Energy Research Instiute: Golden, CO, USA, 1987. Available online: https://www.nrel.gov/docs/legosti/old/3087.pdf (accessed on 28 September 2022).
30. Li, D.H.W.; Cheung, G.H.W. Study of models for predicting the diffuse irradiance on inclined surfaces. *Appl. Energy* **2005**, *81*, 170–186. [CrossRef]
31. Kasten, F. A Simple Parameterization of the Pyrheliometric Formula for Determining the Linke Turbidity Factor. *Meteorol. Rundsch.* **1980**, *33*, 124–127.
32. Kasten, F. A new table and approximation formula for the relative optial air mass. *Arch. Meteorol. Geophys. Bioklimatol. Ser. B* **1966**, *14*, 206–223. [CrossRef]
33. Wright, J.; Perez, R.; Michalsky, J.J. Luminous efficacy of direct irradiance: Variations with insolation and moisture conditions. *Sol. Energy* **1989**, *42*, 387–394. [CrossRef]
34. Perez, R.; Ineichen, P.; Seals, R.; Zelenka, A. Making full use of the clearness index for parameterizing hourly insolation conditions. *Sol. Energy* **1990**, *45*, 111–114. [CrossRef]